Published in final edited form as:
J Theor Biol. 2010 June 21; 264(4): 1225–1239. doi:10.1016/j.jtbi.2010.03.027.

MODEL OF COLONIC INFLAMMATION: IMMUNE MODULATORY MECHANISMS IN INFLAMMATORY BOWEL DISEASE

Katherine Wendelsdorf[1], **Josep Bassaganya-Riera**, **Raquel Hontecillas**, and **Stephen Eubank**
Virginia Bioinformatics Institute, Virginia Polytechnic Institute and University, Washington Street, MC 0477 Blacksburg, Virginia 24061 USA

Abstract

Inflammatory Bowel Disease (IBD) is an immunoinflammatory illness of the gut initiated by an immune response to bacteria in the microflora. The resulting immunopathogenesis leads to lesions in epithelial lining of the colon through which bacteria may infiltrate the tissue causing recurring bouts of diarrhea, rectal bleeding, and mal-nutrition. In healthy individuals such immunopathogenesis is avoided by the presence of regulatory cells that inhibit the inflammatory pathway. Highly relevant to the search for treatment strategies is the identification of components of the inflammatory pathway that allow regulatory mechanisms to be overridden and immunopathogenesis to proceed. *In vitro* techniques have identified cellular interactions involved in inflammation-regulation crosstalk. However, tracing immunological mechanisms discovered at the cellular level confidently back to an *in vivo* context of multiple, simultaneous interactions has met limited success.

To explore the impact of specific interactions, we have constructed a system of 29 ordinary differential equations representing different phenotypes of T-cells, macrophages, dendritic cells, and epithelial cells as they move and interact with bacteria in the lumen, lamina propria, and lymphoid tissue of the colon.

Simulations revealed the positive inflammatory feedback loop formed by inflammatory M1 macrophage activation of T-cells as a driving force underlying the immunopathology of IBD. Furthermore, strategies that remove M1 from the site of infection, by either i) increasing its potential to switch to a regulatory M2 phenotype or ii) increasing the rate of reversion (for M1 and M2 alike) to a resting state, cease immunopathogenesis even as bacteria are eliminated by other inflammatory cells.

Based on these results, we identify macrophages and their mechanisms of plasticity as key targets for mucosal inflammation intervention strategies. In addition, we propose that the primary mechanism behind the association of PPARγ mutation with IBD is its ability to mediate the M1 to M2 switch.

1. Introduction

Inflammatory Bowel Disease (IBD) is a chronic illness of the gut characterized by a recurring inflammatory response to bacteria in the lumen microflora resulting in lesions of the epithelial

[1]Corresponding author: wkath83@vbi.vt.edu .

lining and lamina propria (Swidsinski *et al.*, 2002). The lamina propria is the tissue site where immune cells initially recognize bacterial antigen prior to migrating to the distal lymphoid tissue to mount the inflammatory response. IBD results in two clinical manifestations, Crohns disease and ulcerative colitis, in which the patient experiences relapses of diarrhea, rectal bleeding, and malnutrition as bacteria from the lumen leak into the lamina propria through the lesions in the epithelial barrier (Cho, 2008). Over 1 million people are afflicted by IBD in North America and 4 million worldwide resulting in a severe decrease in quality of life as well as significant health care-related costs (Stenson, 1995). Total expenses exceed $15 billion annually in the U.S. not including indirect expenses of treating complications such as recurrent pancreatitis, abscesses, intestinal obstruction, anemia, thromboses, perianal lesions, arthritis, uveitis, iritis, or cutaneous lesions (Braverman, 2003; Barba *et al*., 2002).

In a healthy individual, immune cells of the gut mucosa remain largely inactive towards the 10^{14} bacteria that compose the microflora. This tolerance to most bacterial strains is attributed to the prominent presence of regulatory immune cells that may be triggered by the commensal microflora and whose functions are antagonistic to inflammatory pathways triggered by small, transient populations of pathogenic bacteria.

For an illustration of immune response pathways in the gut mucosa, please look to Figure 1. The inflammatory pathway portrayed is currently believed to occur as follows: Inflammation is initiated when resting antigen presenting cells, dendritic cells and macrophages, endocytose bacterial antigen at the initial site of infection, the lumen. In the lamina propria (LP), these cells then differentiate to inflammatory or effector phenotypes, termed M1 macrophages (M1) and effector dendritic cells (De) secreting inflammatory mediators including factors that aid infiltration of additional resting macrophage and dendritic cell precursors (monocytes) as well as T-cells into the LP. De and M1 present antigen to resting T-cells while secreting cytokines IL-12, IFN-γ,TNF-α, and IL-23 inducing their differentiation to pro-inflammatory T-helper cells (Th), specifically Th1 or Th17 phenotypes, that also secrete inflammatory mediators (Iwasaki, 2007;Gordon & Taylor, 2005). Antigen presenting cells may also migrate away from the infection site to the lymphoid tissue where they contact and stimulate a larger concentration of T-cells that will, in turn, relocate to the infection site in the lamina propria. There, Th1 and Th17 act synergistically with M1 and De to recruit more monocytes and promote their differentiation to the pro-inflammatory M1 and De phenotypes closing a positive feedback loop.

Immunopathogenesis results from secretion of toxic peroxide anions, proteases, and oxygen/nitrogen radicals by M1 and Th1-activated cells that kill the invading bacteria, but also cause indiscriminate tissue damage. In sterile organ systems, the inflammatory process generally ceases once the antigen population is eliminated and immune cells are no longer stimulated directly. However, in the gut, inflammation induced by bacterial microflora presents a scenario where the antigen population cannot be eliminated allowing the collateral cost of immunopathogensis to mount and become more harmful to the host than the invading bacteria itself. Compounding the problem, inflammation-induced damage to the epithelial barrier between the lumen and lamina propria allows increased permeability and infiltration of bacteria into the lamina propria, thereby allowing heightened macrophage and dendritic cell stimulation completing another positive feedback loop that magnifies the inflammatory responses during IBD (Figure 1).

In healthy individuals, to avoid this occurrence, the gut mucosa contains various regulatory factors such as M2 macrophages (M2), tolerogenic dendritic cells (Dt), and T-regulatory cells that are analogous to, and act antagonistically with, their inflammatory counter parts M1, De, and Th1/ Th17. In the regulatory pathway, binding of ligands recognized as self, including commensal bacteria, to specific surface receptors of resting macrophages and dendritic cells

induce their differentiation to M2 and Dt as opposed to M1 and De. One such receptor is the peroxisome proliferator-activated receptor, PPARγ, expressed in T-cells, dendritic cells, macrophages, and epithelial cells (Spiegelman, 1998; Mansen *et al*., 1996). This process is aided by the presence of anti-inflammatory cytokines IL-10 and TGF-β that inhibit pro-inflammatory cytokine secretion and down-regulation of co-stimulatory molecule expression (Asseman *et al*., 1999). The net result is that, upon antigen presentation by M2 and Dt, resting T-cells differentiate to a T-regulatory phenotypes. These are called *induced* T-regulatory cells (Ti) because their resting precursors have the ability to become Th1 upon stimulation by IFN-γ+IL-12 secreting M1 and De. In contrast, *natural* T-regulatory cells (Tr) are T-cells that are pre-destined to be regulatory cells independent of the cytokine environment. Both Ti and Tr secrete IL-10 and TGF-β promoting further M2 and Dt creation. In addition, Tr has been shown to bind effector dendritic cells with high affinity and inhibit their stimulation of resting T-cells to inflammatory phenotypes (Onishi *et al*., 2008).

In the current biological model of gut homeostasis commensal bacteria-mediated stimulation is largely responsible for upholding the basal population of regulatory factors that inhibit the inflammatory responses of their neighboring cells (Figure 1). This normally allows the presence of a small population of inflammatory immune cells in response to the occasional invasion of pathogenic bacteria while the system remains inactive towards nonpathogenic strains in the microflora that maintain gut function. In abnormal cases, such as IBD, this low-level inflammatory response is able to mount, from an initially small population, to a much larger population able to override the suppressive activity of its regulatory anatagonists. An area of key interest to IBD intervention is identification of the specific interactions of the inflammatory pathway that allow this cascade effect to take hold and subsequent immunopathogenesis to proceed.

Many of the mentioned interactions involved in inflammatory-regulatory crosstalk have been identified *in vitro*. It is yet to be identified which of these *in vitro* observed mechanisms lie behind the immunopathogenic cell dynamics observed *in vivo* during inflammation. For example, IBD recovery is associated with increased levels of T-regulatory cells in animal models (Powrie *et al*., 1993; Hontecillas & Bassaganya-Riera, 2007). Is this due to Trspecific activity, such as the direct disruption of De-mediated T-cell stimulation, or its role as one of many IL-10 secreting cells, which could have numerous downstream effects?

There is still no cure for IBD and the only available treatments include those that universally weaken mucosal immunity leaving the patient vulnerable to opportunistic pathogens (Bassaganya-Riera *et al*., 2004). Identifying the specific regulatory functions that mediate the chronic inflammatory response would provide new strategies for more sophisticated treatment options.

Towards this goal we have developed a system of 29 ordinary differential equations describing the movement, interaction, and activation of inflammatory regulatory macrophages, T-cells, and dendritic cells in the presence of bacteria and cytokines in the lumen, lamina propria, and lymphoid tissue regions of gut mucosa. *In silico*, we induced chronic inflammation by allowing resting macrophages and dendritic cells to differentiate to inflammatory phenotypes upon contact with bacteria of the microflora. We then traced dynamics of inflammation markers back to specific interactions identifying those that override regulatory factors and sustain an immunopathogenic inflammatory response.

2. Methods

2.1. Mathematical model

Our model describes population dynamics of immune cells and epithelial cells as they interact, flow, and differentiate over time in response to dynamic populations of cytokines and bacteria (Figure 2). The populations are further compartmentalized by three locations between which the cells may migrate: i) the lumen, where bacteria reside, which is denoted by the superscript 'L' ii) the lamina propria, more generally termed the *effector* site of the immune response, denoted by the superscript 'E' and iii) the mesenteric lymph node, the *inductive* site of the immune response, denoted by the superscript 'I'. In the following equations capital roman letters denote variables, lowercase and greek letters denote parameters, and subscripts the cell phenotype. An organized list of model parameters and their corresponding symbols is given in Appendix A. A list of the variables is given in Appendix B.

Cytokines—Some parameter values are dependent on cytokine levels. The model includes an activating cytokine group, C_a, in the inductive site (Equation 1) and effector site (Equation 2) that represents factors secreted by inflammatory phenotypes including IFN-γ, TNF-α , pro-inflammatory cytokines, proteases and free radicals such as nitric oxide. The second group is deactivating cytokines, C_d, representing IL-10 and TGF-β (Equations 3 and 4). As a simplifying assumption, the different cytokines are secreted at the same constant rate, λ_c, from active cells of different phenotypes and degrade at a constant rate, μ_c. This decision was reinforced by a lack of significant sensitivity of immune cell population levels to these particular parameters.

$$\frac{dC_a^I}{dt}=\lambda_c\left(T_h^I+D_e^I\right)-\mu_c C_a^I \tag{1}$$

$$\frac{dC_a^E}{dt}=\lambda_c\left(T_h^E+M_1^E+D_e^E+E_p\right)-\mu_c C_a^E \tag{2}$$

$$\frac{dC_d^I}{dt}=\lambda_c\left(T_i^I+T_r^{I*}+D_t^I\right)-\mu_c C_d^I \tag{3}$$

$$\frac{dC_d^E}{dt}=\lambda_c\left(T_i^E+T_r^{E*}+M_2^E+D_t^E\right)-\mu_c C_d^E \tag{4}$$

Bacteria—Equations 5 and 6 represent bacteria in the lumen and lamina propria compartments, respectively, where λ_b, ϕ_b, and μ_b are birth rate, crowding co-efficient, and death rate. In the healthy model, this population is largely composed of *commensal* bacteria. Bacteria may migrate from the lumen to the lamina propria at a rate, ϵ_{LE}, where $\epsilon_{LE}=\left(\frac{C_a^E}{qC_a^E+E+E_p}\right)^{y_\epsilon}$. Note that this function evaluates to 0 in the absence of activating cytokines (C_a^E), increasing as C_a^E concentration rises and the epithelial cell concentration ($E + E_p$) falls. This represents epithelial cell modification by pro-inflammatory cytokines, which increases permeability and lesion formation (Yang *et al.*, 2003). The parameter q controls the cytokine level at which migration occurs and y_ϵ is the rate at which the bacterial migration increases with respect to

C_a^E and $E + E_p$ levels. Bacteria are eliminated by inflammatory epithelial cells (E_p) and M1 macrophages (M_1^E), which secrete microbicides, as well as uptake by resting antigen presenting cells (M_0^E, D_i^E, and D_i^L). This is represented by the terms $k_L\left(E_p+D_i^L\right)$ in equation 5 and $k\left(E_p+M_1^E+M_0^E+D_i^E\right)$ in equation 6 where k_L and k are contact rates between individual cells in the lumen and lamina propria, respectively.

$$\frac{dB_c^L}{dt}=B_c^L\left(\lambda_b-\Phi_b B_c^L-\mu_b-k_L\left(E_p+D_i^L\right)-\epsilon_{LE}\right) \tag{5}$$

$$\frac{dB_c^E}{dt}=B_c^E\left(\lambda_b-\Phi_b B_c^E-\mu_b-k\left(E_p+M_1^E+M_0^E+D_i^E\right)\right)+B_c^L\epsilon_{LE} \tag{6}$$

Epithelial Cells—Equation 7 describes the dynamics of cells of the epithelial lining as they replicate and die at constant rates, λ_E and μ_E respectively. The parameter ϕ_E is a crowding co-efficient that allows population growth to cease at the healthy basal concentration of 10^4/mL (Artis, 2008), representing an intact barrier composed of normal epithelial cells (E) as well as cytokine-secreting pro-inflammatory epithelial cells (E_p). The term $\nu_{EC}C_a^E$ represents transition of an epithelial cell to a *pro-inflammatory* epithelial cell, E_p, described in equation 8. This represents the ability of cytokines encompassed in the activating group to induce secretion of pro-inflammatory mediators by epithelial cells(Artis, 2008). The term $\mu_{ce}C_a^E$ in equation 8 represents death induced by cytopathic factors, also present in the activating cytokine group. The assumption here is that the same pathways that lead to factors that stimulate epithelial cells to secrete cytokines, such as IFN-γ, are coupled with those that produce free radicals and proteases.

$$\frac{dE}{dt}=E\left(\lambda_E-\Phi_E\left(E+E_p\right)-\mu_E-\nu_{EC}C_a^E\right)+\mu_E E_p \tag{7}$$

$$\frac{dE_p}{dt}=\nu_{EC}EC_a^E-E_p\left(\mu_E+\mu_{ce}C_a^E\right) \tag{8}$$

Dendritic Cells—Immature dendritic cells are present in the lamina propria (D_i^E, Equation 9), of which a subset are localized to the epithelial barrier allowing dendrites to extend through epithelial cells into lumen to contact bacteria (Iwasaki, 2007). This subset is represented as dendritic cells in the lumen compartment (D_i^L, Equation 11). The immature dendritic cell population is fed by monocytes from the blood at rates λ_d (Equation 10) and λ_{dl} (Equation 12) such that each D_i^E that transfers to one of the activated dendritic cell compartments is replaced with a net increase of the population in the presence of inflammatory cytokines (Janeway *et al*., 2001). This increase occurs with the term $\epsilon_r C_a^E$, which represents general recruitment of leukocytes by inflammatory mediators encompassed in the activating cytokine group and is applied to all resting cell populations in the model (Janeway *et al*., 2001). The recruitment rate, ϵ_r, is likely different for each resting cell population, but we make the assumption of one parameter value for all populations.

The D_i^L population is assume to be determined by the limited space near the epithelial barrier that can be occupied, which would not increase with the amount of inflammatory cytokines, C_a. This population, therefore, remains constant even under inflammatory conditions.

Upon contact with bacteria, a cell of the D_i^E or D_i^L population becomes either an effector dendritic cell (D_e^E, Equation 13), with the probability v_{Bc}, or tolerogenic dendritic cell (D_t^E, Equation 14) where v_{Bc} is the fraction of commensal bacteria that induces an inflammatory phenotype. In a healthy person, this should be negligible and is set to a value of 0. After a period in the lamina propria, corresponding to the migration rate ϵ_{EI}, the presenting dendritic cells migrate to the lymph node joining the D_e^I and D_t^I populations. Here they can stimulate resting T-cells until they die at a rate of μ_d.

The terms $k_T T_r^{E*}$ in equation 13 and $k_T T_r^{l*}$ in equation 15 represent contact with active natural T-regulatory cells in the effector and inductive sites respectively. Upon contact with active natural T-regulatory cells, effector dendritic cells are rendered anergic, unable to secrete activating cytokine or stimulate resting T-cells (Onishi *et al*., 2008). We represent this by effectively removing them from the system upon contact with active T-regulatory cells (T_r^{E*} and T_r^{l*}). k_T is the contact rate between antigen presenting cells and T-regulatory cells. This is set to be greater than the contact rates between all other cells, k, due to evidence that natural T-regulatory have a higher affinity for dendritic cells than do conventional T-cells (Onishi *et al*., 2008).

$$\frac{dD_i^E}{dt} = \lambda_d + \epsilon_r C_a^E - D_i^E \left(kB_c^E + \mu_{di}\right) = \epsilon_r C_a^E \tag{9}$$

$$\lambda_d = D_i^E \left(kB_c^E + \mu_{di}\right) \tag{10}$$

$$\frac{dD_i^L}{dt} = \lambda_{dl} - D_i^L \left(k_L B_c^L + \mu_{di}\right) = 0 \tag{11}$$

$$\lambda_{dl} = D_i^L \left(k_L B_c^L + \mu_{di}\right) \tag{12}$$

$$\frac{dD_e^E}{dt} = D_i^E \left(k\nu_{Bc} B_c^E\right) + D_i^L \left(k_L \nu_{Bc} B_c^L\right) - D_e^E \left(\epsilon_{EI} + k_T T_r^{E*}\right) \tag{13}$$

$$\frac{dD_t^E}{dt} = D_i^E \left(k\left(1 - \nu_{Bc}\right) B_c^E\right) + D_i^L \left(k_L \left(1 - \nu_{Bc}\right) B_c^L\right) - \epsilon_{EI} D_t^E \tag{14}$$

$$\frac{dD_e^I}{dt}=\epsilon_{EI}D_e^E - D_e^I\left(k_T T_r^{I*}+\mu_d\right) \tag{15}$$

$$\frac{dD_t^I}{dt}=\epsilon_{EI}D_t^E - \mu_d D_t^I \tag{16}$$

Macrophages—Undifferentiated, resting M0 macrophages (M_0^E, Equation 17) are only represented in the lamina propria and not the mesenteric lymph node. This is under the assumption that, due to compartmentalization of a typical lymph node, the impact of macrophage-derived cytokines on T-cell differentiation is negligible compared to that of the dendritic cell-derived cytokines. Observations that macrophages participate primarily in plasma B-cell differentiation support this assumption (Junt *et al*., 2007; Mohr *et al*., 2009). The M_0^E population is fed by monocytes from the blood at the rate λ_m (Equation 18). Similar to the function for immature dendritic cell replenishment (λ_d, Equation 9), λ_m is a function that allows replacement of each M_0^E transferred to one of the activated macrophage pools from an implied, unlimited monocyte pool with a net increase of $\epsilon_r C_a^E$. Upon contact with bacteria that manages to invade from the lumen, a M0 becomes a M1 macrophage (M_1^E, Equation 19) or M2 macrophage (M_2^E, Equation 20) and secretes activating or de-activating cytokine for the period of activation. This is represented by the terms $kM_0^E\nu_{Bc}B_c^E$ in equation 19 and $kM_0^E\left(1-\nu_{Bc}\right)B_c^E$ in equation 21. As mentioned, ν_{Bc} is the fraction of commensal bacteria that induces an inflammatory phenotype and is set to 0.

Macrophages may switch phenotypes as the cytokine ratio changes in the lamina propria so that M1 switches to M2 with a probability proportional to the C_d/C_a ratio and M2 switches to M1 with a probability proportional to the C_a/C_d ratio. This is represented by the terms $\nu_{21}=\frac{C_a}{C_d+C_a}$ and $\nu_{12}=\frac{C_d}{C_d+C_a}$ in equations 19 and 20 respectively . The term $\nu_{M0}\left(M_1^E+M_2^E\right)$ represents reversion of activated macrophages back to the resting state at a rate of ν_{M0}, a process believed to play a role in quelling inflammation once pathogen is eliminated. Though reversion is determined by environmental factors that change dynamically as the immune response progresses (Gordon & Taylor, 2005), we treat this parameter as a constant for the sake of simplification. In the absence of an experimental measurement we initially set ν_{M0} to a value of 0. Neither calibration (discussed below in section 2.3) nor validation (section 2.4) of the model indicated a need to include this mechanism in order to observe characteristic cessation of inflammation. This may be interpreted as a model assumption that the frequency of reversion to an inactive state is negligible.

Macrophage lifespan is also dynamic and may be tissue dependent. We also assume this parameter to be a constant for the sake of simplicity, corresponding to the rate μ_m.

$$\frac{dM_0^E}{dt}=\lambda_m+\epsilon_r C_a^E+\nu_{M0}\left(M_1^E+M_2^E\right) - M_0^E\left(kB_c^E+\mu_m\right)=\epsilon_r C_a^E \tag{17}$$

$$\lambda_m=M_0^E\left(kB_c^E+\mu_m\right) - \nu_{M0}\left(M_1^E+M_2^E\right) \tag{18}$$

$$\frac{dM_1^E}{dt} = kM_0^E \nu_{Bc} B_c^E + M_2^E \nu_{21} - M_1^E (\nu_{M0} + \nu_{12} + \mu_m) \tag{19}$$

$$\frac{dM_2^E}{dt} = kM_0^E (1 - \nu_{Bc}) B_c^E + M_1^E \nu_{12} - M_2^E (\nu_{M0} + \nu_{21} + \mu_m) \tag{20}$$

T-cells in the inductive site—The model includes two resting T-cell populations in the mesenteric lymph node, naive T-cells (T_n, Equation 21) and *central* memory T-cells (T_c, Equation 22). Naive and central memory T-cells may flow in and out of the lymph node at constant rates λ_t and μ_t, but not to the effector site of the lamina propria (Sallusto *et al*., 2004; Janeway *et al*., 2001). They may also be recruited by inflammatory factors in the lymph node, represented by the term $\epsilon_r C_a^I$.

Resting T-cells contact antigen presenting dendritic cells and may be stimulated with a probability, α_t or α_T, meant to encompass the probability that the antigen presented is recognized by the specific T-cell. This is represented by the terms $T_n k\alpha_t \left(D_e^I + D_t^I\right)$ and $T_c k\alpha_T \left(D_e^I + D_t^I\right)$, where k is the same cell contact rate as in the effector site. The probability of stimulation of a memory T-cell, α_T, is greater than that for a naive T-cell, α_t, as memory T-cells have less stringent antigen specificity (Janeway *et al*., 2001). Upon stimulation, the resting T-cell enters either the active T-helper cell pool (T_h, Equation 23) or induced T-regulatory pool (T_i, Equation 24) depending on the dendritic cell phenotype (Iwasaki, 2007). T_h secretes activating cytokine and T_i secretes deactivating cytokine. Upon creation in the inductive site, these cells proliferate at a rate of p_t. After a 48 hour maturation period, corresponding to the rate ϵ_{IE}, the T-cell will migrate to the effector site(Janeway *et al*., 2001). Note that this rate is applied to each active T-cell population as a whole, which does not allow migration to be specific to recently matured T-cells. Rather, the terms $-T_h^I \epsilon_{IE}$ and $-T_i^I \epsilon_{IE}$, taken from equations 23 and 24, apply an exponential distribution of residence times with an average of 48 hours over all active T-cells. This simplification strategy was chosen over the use of a delay term, which would be more biologically accurate, but at the cost of a significantly more complicated set of equations.

The term $0.6\nu_T \mu_T \left(T_h^E + T_i^E\right)$ in equation 22 represents the fraction of active T-cells that become central memory T-cells once de-activated in the effector site. The parameter μ_T is the rate of de-activation and ν_T is the fraction that revert to resting state. Roughly 60% of these de-activated T-cells will be central memory T-cells and the rest will go on to be effector memory T-cells (T_E), represented in equation 25 and discussed below(Sallusto *et al*., 2004; Marzo *et al*., 2005).

$$\frac{dT_n}{dt} = \lambda_t + \epsilon_r C_a^I - T_n \left(k\alpha_t \left(D_e^I + D_t^I\right) + \mu_t\right) \tag{21}$$

$$\frac{dT_C}{dt} = \lambda_t + 0.6\nu_T \mu_T \left(T_h^E + T_i^E\right) + \epsilon_r C_a^I - T_C \left(k\alpha_t \left(D_e^I + D_t^I\right) + \mu_t\right) \tag{22}$$

$$\frac{dT_h^I}{dt}=k\alpha_t T_n D_e^I+k\alpha_t T_c D_e^I+T_h^I(p_t-\epsilon_{IE}) \tag{23}$$

$$\frac{dT_i^I}{dt}=k\alpha_t T_n D_t^I+k\alpha_t T_c D_t^I+T_i^I(p_t-\epsilon_{IE}) \tag{24}$$

T-cells in the effector site—Equation 25 represents the resting *effector* memory T-cell population in the lamina propria (T_E). This is a subset of memory T-cells that only circulate in peripheral tissues distinct from central memory T-cells that circulate among lymphoid tissue. Memory T-cells enter and exit the LP via the blood at rates ϵ_{BE} and ϵ_{EB} respectively. The rate at which memory T-cells infiltrate the tissue from the blood is assumed to be independent of the current tissue concentration, T_E. Once in the tissue, T_E is in contact with both presenting macrophages and dendritic cells and may be stimulated with a probability of α_T under the assumption that the antigen specificity is generally the same as for central memory T-cells. The term $0.4\nu_T\mu_T\left(T_h^E+T_i^E\right)$ represents the fraction of de-activated T-cells that become effector memory T-cells.

Equations 26 and 27 represent inflammatory T-helper cells (T_h^E) and induced T-regulatory cells (T_i^E) in the lamina propria. A stimulated T_E enters one of these two pools depending on the phenotype of antigen presenting cell represented by the terms $k\alpha_T T_E\left(D_e^E+M_1^E\right)$ in equation 26 and $k\alpha_T T_E\left(D_t^E+M_2^E\right)$ in equation 27. Upon stimulation of effector memory T-cells, the resulting active T-cells (T_h^E and T_i^E)proliferate at a lower rate, p_T, than those born from naive and central memory T-cells, p_t (Geginat *et al*., 2003). The term $\epsilon_{IE}T_h^I$ and $\epsilon_{IE}T_i^I$ represent infiltration of T-cells activated in the inductive site into the effector site.

$$\frac{dT_E}{dt}=\epsilon_{BE}+0.4\nu_T\mu_T\left(T_h^E+T_i^E\right)+\epsilon_r C_a^E-T_E\left(k\alpha_t\left(D_e^E+D_t^E+M_1^E+M_2^E\right)+\epsilon_{EB}\right) \tag{25}$$

$$\frac{dT_h^E}{dt}=\epsilon_{IE}T_h^I+k\alpha_t T_E\left(D_e^E+M_1^E\right)+T_h^E(p_t-\mu_T) \tag{26}$$

$$\frac{dT_i^E}{dt}=\epsilon_{IE}T_i^I+k\alpha_T T_E\left(D_t^E+M_2^E\right)+T_i^E(p_T-\mu_T) \tag{27}$$

Natural T-regulatory cells—Equation 28 describes resting natural T-regulatory cells as they enter and exit the effector site via the blood. As with effector memory T-cells, resting natural T-regulatory cells are assumed to infiltrate the tissue with a rate that is independent of the concentration of cells already in the tissue site. At the infection site, Tr are stimulated by antigen presenting cells of both inflammatory and regulatory phenotypes. This interaction is represented by the term $k_T\alpha_T\left(D_e^E+D_t^E+M_1^E+M_2^E\right)$, where we assume a stimulation rate that is the same as other memory T-cells, α_T. A stimulated cell then becomes an *active* natural T-

regulatory cell (T_r^{E*}, Equation 29). T_r^{E*} cells migrate from the effector site to the inductive site via draining lymph, entering the T_r^{I*} population (Equation 30). Here they carry out their primary regulatory function by inhibiting effector dendritic cell stimulation of T-cells, represented in equations 13 and 15 (Shevach, 2002; Onishi *et al*., 2008). While activated, the cell proliferates at a rate of p_{Tr}. Calibration of p_{Tr} such that the CD4+ T-cell concentration in the lymph node stays within measured ranges *in vivo* (Haase, 1999) lead to a lower value than for the proliferation rate of conventional T-cells, p_t. This decreased proliferation rate is supported by the fact that Tr expresses decreased levels of IL2R compared to helper T-cells (Walker *et al*., 2003). We assume the rate of deactivation for natural T-regulatory cells is the same for induced T-regulatory cells, μ_T, as is the fraction that revert back to the resting state as opposed to undergoing apoptosis, ν_T.

$$\frac{dT_r^E}{dt}=\epsilon_{BE}+\epsilon_r C_a^E+\mu_T \nu_T T_r^{1*} - T_r^E\left(k_T \alpha_T \left(D_e^E+D_t^E+M_1^E+M_2^E\right)-\epsilon_{EB}\right) \tag{28}$$

$$\frac{dT_r^{E*}}{dt}=T_r^E\left(k_T \alpha_T \left(D_e^E+D_t^E+M_1^E+M_2^E\right)\right)+pT_r T_r^{E*} - \epsilon_{EI} T_r^{E*} \tag{29}$$

$$\frac{dT_r^{I*}}{dt}=\epsilon_{EI} T_r^{E*}+T_r^{I*}\left(p_{T_r}-\mu_T\right) \tag{30}$$

2.2. Simulations

The system of differential equations was solved using the LSODA algorithm in COPASI (Hoops *et al*., 2006). The system was solved over 3000 time units, where one time unit, *t*, is approximately 6 hours. During calibration, transition rates were estimated based on this time scale. However, due to uncertainty in the rates, it is best to view the system as a model of qualitative dynamics. We, therefore, do not seek to make any temporal predictions based on model time.

2.3. Sensitivity analysis

Sensitivities of each variable to each parameter of the model was determined in COPASI. For this task COPASI uses metabolic control analysis (MCA), a method developed to carry out sensitivity analysis of metabolic systems. In short, MCA studies the relative control exerted by each step on the system's variables by applying a perturbation to the step being studied and then measuring the effect on the variable of interest after the system has settled to a new steady state. For a more in depth description please refer to Reder *et al*.(Reder, 1988).

2.4. Parameter assignment and model calibration

Parameter values for a healthy individual were gathered from literature, where possible, using mouse, pig, and human data (Appendix A). Unknown parameters were approximated with expert knowledge or estimated from a range. In some cases optimization was carried out in COPASI using the particle swarm algorithm.

The model was calibrated to fit specific criteria for gut homeostasis in the absence of foreign bacteria at steady-state (Figure 3A). The criteria included: *i*) T-cell numbers reflect those measured in lymphoid tissue of healthy individuals. Specifically, concentrations of naive T-cells and memory T-cells are approximately $1.2{\cdot}10^8$/mL in the lymph node(Haase, 1999) and

dendritic cells are 10^6/mL (Catron *et al*., 2004). *ii*) No commensal bacteria is seen in the lamina propria, but the lumen population upholds a regulatory immune cell population. *iii*) The lumen bacteria stays within a concentration of $10^{11} – 10^{12}$/mL (Artis, 2008). *iv*) The epithelial cell layer remains unchanged from an initial concentration of 10^4/mL (Artis, 2008). *v*) Active and resting natural T-regulatory cells compose approximately 10% of the total CD4+ T-cell population (Asano *et al*., 1996). *vi*) The level of deactivating cytokine-secreting cells in the lamina propria are significantly higher than activating cytokine-secreting cell levels (Uhlig *et al*., 2006). The system was deemed to have converged when the relative change in concentration in a single time step was less than 10^{-5}.

A more detailed explanation of parameter assignment and range estimation is given in Appendix A.

2.5. Validation

To validate the model, we sought to replicate cell dynamics observed in pigs experimentally infected with pathogenic bacteria strains (Hontecillas *et al*., 2005; Jonasson *et al*., 2006). To do this we added a pathogenic bacterial population (Bf), recognized by antigen presenting cells as *foreign*, to the model. In this extended model, the Bf population induces inflammatory phenotypes in resting dendritic cells and macrophages upon contact and act competitively with commensal bacteria. Specifically, the extension involves slight modifications to equations for resting macrophages (M_0^E, Equation 17) and activated macrophages (M_1^E and M_2^E, Equations 19 and 21) by replacing the terms $M_0^E\left(kB_c^E+\mu_m\right)$ in equation 17, $kM_0^E\nu_{Bc}B_c^E$ in equation 19, and $kM_0^E\left(1-\nu_{Bc}\right)B_c^E$ in equation 20 with $M_0^Ek\left(B_c^E+B_f^E\right)$, $kM_0^EB_f^E$, and $kM_0^EB_c^E$ respectivley. B_f^E represents the concentration of foreign bacteria in the effector site. The terms assume that all contact events with foregin bacteria lead to an inflammatory M1 phenotype and those with commensal bacteria lead to a tolerogenic M2 phenotype. With these same assumptions applied to dendritic cells the terms kB_c^E in equations 9 and 10, $k_LB_c^L$ in equations 11 and 12, $D_i^E\left(k\nu_{Bc}B_c^E\right)+D_i^L\left(k_L\nu_{Bc}B_c^L\right)$ in equation 13, and $D_i^E\left(k\left(1-\nu_{Bc}\right)B_c^E\right)+D_i^L\left(k_L\left(1-\nu_{Bc}\right)B_c^L\right)$ in equation 14 are replaced with the terms $k\left(B_c^E+B_f^E\right)$, $k_L\left(B_c^L+B_f^L\right)$, $D_i^EkB_f^E+D_i^Lk_LB_f^L$ and $D_i^EkB_c^E+D_i^Lk_LB_c^L$ respectivley. Equations 31 and 32 describe interdependent dynamics of the competing bacterial populations. All parameters are considered identical between the two populations, where γ is a competition coefficient. The full equations of these populations directly affected by the introduction of foreign bacteria are given in Supplementary Materials.

$$\frac{dB_c}{dt}=B_c\left(\lambda_b-\phi_BB_c-\gamma B_f-\mu_b\right) \tag{31}$$

$$\frac{dB_f}{dt}=B_f\left(\lambda_b-\phi_BB_f-\gamma B_c-\mu_b\right) \tag{32}$$

The model was validated by adding the presence of foreign bacteria with these modification and initiating simulations with a Bf concentration of 10^8/mL in the lumen. Under these conditions, the model produced the same qualitative population dynamics as those in the animal studies carried out by Hontecillas et al. (Hontecillas *et al*., 2005) and Jonas-son et al. (Jonasson *et al*., 2006) (Figure 3B). Specifically; *i*) The most significant cell population increase is among inflammatory phenotypes. *ii*) Inflammation coincided with a depletion of the epithelial cell layer by 2%. *iii*) Inflammation and epithelial cell depletion coincided with an increased rate of

bacterial migration across the epithelial barrier and accumulation in the lamina propria. *iv*) Inflammation coincided with an increased rate of M2 macrophages switching to M1 *v*) Recovery was observed coinciding with reversion of all macrophages back to M2, return of the epithelial cell concentration to the basal level, reduction of inflammatory cell types to near homeostatic levels (concentration of < 1 in the case of cells and < 10 in the case of activating cytokines), and elimination of bacteria from the lamina propria.

2.6. IBD model

To induce IBD in the model of healthy mucosa, we changed the parameter v_{Bc}, the rate of M_0 or D_i^E transition to D_e or M_1 upon contact with bacteria of the microflora, from 0 to increasingly positive values. IBD was defined as a new steady-state in which there is an increased level of inflammatory markers including activating cytokines (Ca), T-helper cells (Th), M1 macrophages (M1), and effector dendritic cells(De) in conjunction with decreased epithelial cell concentration (E+Ep), representing chronic lesion presence. A positive value for v_{Bc} could represent a number of plausible causes of IBD such as: *i*) Impairment of the regulatory pathway in antigen-presenting cells where the default is the inflammatory pathway; *ii*) Dysfunction of specific pattern recognition receptors leading to recognition of residential bacteria as foreign; *iii*) Change in composition of the residential bacterial population, i.e. microflora imbalance. The latter is associated with IBD in the literature (Ott *et al*., 2004; Swidsinski *et al*., 2002).

3. Results

3.1. Impairment of antigen presenting cell tolerance pathways causes IBD

Commensal bacteria should not induce inflammatory phenotypes in dendritic cells or macrophages, De or M1, in a healthy individual (Strober *et al*., 2002). For this reason, in the healthy model we set the rate of this occurrence, v_{Bc}, to 0 causing all immature dendritic cells and resting macrophages to enter the tolerogenic dendritic cell and M2 macrophage pools upon stimulation by bacteria of the microflora, assumed to be commensal. To represent a dysfunctional regulatory pathway or a microfloral imbalance, we set v_{Bc} to values greater than 0 and observed cell dynamics. When $v_{Bc} = 0.0001$ a new steady-state is reached in which populations of inflammatory cells and activating cytokine remain above homeostatic levels and epithelial cell concentration remains roughly 50% reduced even after elimination of bacteria from the lamina propria compartment. These are characteristics of chronic inflammation as observed in IBD. With this model of IBD, we next sought to determine the mechanism by which the inflammatory cytokine population was held above homeostatic levels, thereby increasing epithelial erosion.

3.2. Significance of macrophage plasticity in chronic inflammation triggered by the gut microflora

Macrophage phenotypes are highly plastic. When IL-10 is present, inflammatory M1 macrophages may differentiate to regulatory M2 macrophages. Similarly, in the presence of IFN-γ and TNF-α, a M2 may convert to a M1 (Gordon & Taylor, 2005). To capture this behavior in our model we set the rate at which activating cytokine-secreting M1 switches to deactivating cytokine-secreting M2, v_{12}, and the rate of M2 to M1, v_{21}, as functions of cytokine levels shown here in equations 33 and 34:

$$v_{12} = \left(\frac{\epsilon C_d}{\epsilon C_d + C_a} \right)^{y_v} \tag{33}$$

$$\nu_{21}=\left(\frac{C_a}{\epsilon C_d+C_a}\right)^{y_\nu} \tag{34}$$

C_d is the concentration of deactivating cytokines and C_a the concentration of activating cytokines in the location compartment. The parameter ϵ controls the threshold ratios of cytokine concentrations at which the macrophage population switches from one phenotype to the other. Specifically, the lower the value of ϵ, the higher the C_d/C_a ratio must be to induce the M1 to M2 switch. The parameter y_ν determines the change in the rate at which the phenotype transition occurs with respect to the changing environmental cytokine ratio by determining the gradient at which the function moves between 0 and 1. Both ϵ and y_ν have values of 1 in the healthy and IBD models. In the IBD model (Figure 4A), sensitivity analysis revealed that all immune cells were more sensitive to these parameters than to any other in the model, with the concentration of M1 being negatively correlated to both, as would be expected. This indicates that the observed cell dynamic, i.e. heightened inflammation, is largely dependent on the switch between M1 and M2. Indeed, mutations that inhibit the activity of the receptor PPARγ, which is involved in induction of M2-associated genes and suppression of M1-associated genes, are significantly linked with clinical IBD (Odegaard *et al*., 2007; Dubuquoy *et al*., 2003).

When ϵ was increased from 1 to 2, the system showed rapid epithelial cell recovery coupled with severe reduction in inflammatory markers, Ca and Th, in the LP (Figure 4B). This change represents a decreased sensitivity of the M2 population to pro-inflammatory cytokines in terms of induction of M1-associated genes and suppression of genes conferring its regulatory capacities. A very similar pattern was seen when y_ν was increased to 2 (data not shown), which could represent a quicker switch back to M2 as inflammatory IFN-γ and TNF-α levels decrease with antigen elimination. We choose to focus on the effects of the parameter ϵ, however, as it is directly translatable to the biological system in terms of cytokine presence and receptor availability, factors readily manipulated in a laboratory setting. Under these rescue conditions, activating cytokine and Th levels remain above homeostatic levels in conjunction with De (not shown) keeping the bacterial population at 0 in the lamina propria compartment. Yet, in the absence of M1, the inflammatory response shown in Figure 4B is not coupled with immunopathogenesis, i.e. the total epithelial cell concentration is maintained at the homeostatic level eventhough effector cell concentrations are higher than homeostatic levels and bacteria is successfully eliminated from the LP. The model, therefore, indicates that removal of M1 from the system should allow epithelial cell recovery even in the face of an effective inflammatory response to residential bacteria.

Following this hypothesis, we also attempted to rescue the system from IBD by allowing activated macrophages to return to a resting state. Activated macrophages are known to revert to their undifferentiated precursor, M0, in the absence of specific chemokines, cytokines and survival factors (e.g., IL-12, IL-6, TNF-α , Monocyte Chemotactic Protein-1, and Macrophage Colony-Stimulating Factor) secreted during the immune response to bacteria (Yona & Gordon, 2007). In our initial, healthy model this reversion rate, ν_{M0}, is set to 0 as an experimental measurement was not available and the function was not necessary for recovery from severe dysentery in the validation step (section 2.4). In the IBD model, setting this reversion rate to > 0.015 allows eventual recovery over a period of time inversely proportional to the parameter value (Figure 4C).

3.3. M1 is a key component of the inflammatory loop including Th and immune cell precursors in the lamina propria

In the case of relatively large values of ν_{Bc} (> 0.01), the cell populations that showed growth over time proportional to the activating cytokine population were the helper T-cells (Th)

specifically in the lamina propria location, M1 macrophages (M1), resting macrophages (M0), and effector memory T-cells (TE), also in the lamina propria (Figure 5). This indicates that the mechanism of M1 driven hyper-inflammation and immunopathogenesis lies in the particular positive feedback loop for activating cytokine production that involves its secretion by helper T-cells in the lamina propria (highlighted in Figure 2). Specifically, as Ca levels in the lamina propria rise via secretion by Th and M1, there is an increased recruitment of effector memory T-cells (TE) and M0. The additional M0 cells generate M1 via microfloral bacteria stimulation which leads to greater Th creation from the increasing TE pool. Both newly created Th and M1 cells secrete more activating cytokines, thereby closing the loop.

We tested the effect of disrupting this loop under two scenarios. In the first we reduced the rate, ϵ_r, at which TE and M0 cells are recruited by activating cytokines by a factor of 10. This represents integrin inhibition, a proposed treatment of inflammation disorders (Rutgeerts *et al*., 2009). Simulations showed that reduced recruitment actually exacerbated immunopathogenesis with a 29% reduction in the already-depleted epithelial layer and a 17% increase in activating cytokine levels in the LP. Though a lower ϵ_r intuitively leads to fewer inflammatory cell precursors at the site of the infection initially and, therefore, reduced Ca levels, it also leads to a delay in an effective immune response allowing the small amount of bacteria that is in the LP to proliferate to a larger number ultimately eliciting inflammatory responses from a greater number of cells as they eventually enter the tissue at a slower rate.

In the second scenario, we removed the ability of antigen presenting cells to stimulate memory T-cells by setting the rate of stimulation upon contact, α_T, to 0. This removed ability of macrophages and dendritic cells of either phenotype to stimulate memory T-cells (Equations 22 and 25). Removal of this mechanism did little to ameliorate chronic inflammation. Though Ca levels were reduced by 33%, the epithelial layer remained depleted by 40% from homeostatic levels. However, when we removed M1 and De-mediated stimulation, specifically (i.e. leaving Dt and M2-mediated stimulation intact), we see complete return to a healthy state in which Ca levels are reduced by > 99.9%, bacteria is completely removed from the LP, and the epithelial cell concentration is completely restored. The reason for this is that removal of memory T-cell simulation by both phenotypes resulted not only in reduced Th and activating cytokine levels, but also reduced Ti and deactivating cytokine levels. This reduction in the deactivating cytokine concentration in proportion to that in the activating cytokine concentration returns a C_a/C_d ratio that still upholds a pathogenic value for the M2 to M1 switch rate, ν_{21}. Removal specifically of M1 and De-mediated stimulation, however, only leads to a reduction in Th and, subsequently, Ca levels lowering the C_a/C_d ratio and reducing the rate of the M2 to M1 transition. Hence, inhibition of memory T-cell stimulation may be an effective intervention of hyperinflammation and immunopathogenesis, but only if it is specifically targeted to M1 and De-mediated stimulation while leaving M2 and Dt capable of associating with and stimulating memory T-cells.

3.4. Tr mechanisms were ineffective in rescuing the system from IBD

To assess the overall impact of natural T-regulatory cells we eliminated them altogether from the healthy system and found that recovery from colitis was still seen, though it was delayed. This indicates that the mechanisms of Tr activity included in the model, e.g. secretion of IL-10 and TGF-β and removal of effector dendritic cells, would not be sufficient to account for its ability to inhibit acute inflammation, in the case of dysentery, or allow recovery from chronic colitis, as seen in animal studies (Riley *et al*., 2009).

4. Conclusions

Our objective is to understand the critical interactions between the two competing pathways, inflammation and tolerance, that uphold gut homeostasis in healthy individuals. We focus on

those mechanisms of inflammatory and regulatory pathway crosstalk that mediate IBD-like chronic inflammation. Though the underlying cell interactions have been characterized *in vitro*, their net effects in the context of complex immunological networks of dynamic populations is still unknown. In this study we took a systems approach to investigate consequences of these interactions in a simulated *in vivo* context of the gut mucosa comprised of the lumen, lamina propria, and mesenteric lymph node.

We simulated IBD caused by an inflammatory response to microfloral bacteria. Analysis identified M1 as a main culprit of unregulated inflammation and key target for IBD therapy, specifically by intervention at points of macrophage plasticity. This conclusion is supported by previous predictions that the M2 to M1 switch has a significant influence on tuberculosis pathogenesis in the lungs (Day *et al*., 2009). The result advises further research into rescue strategies that remove M1 from the site of infection by either *i*) increasing its potential to switch to M2 or *ii*) increasing the rate of reversion (for M1 and M2 alike) to a resting state.

PPARγ is a cell receptor expressed on T-cells, macrophages, dendritic cells, and epithelial cells that has been implicated in IBD prevention (Spiegelman, 1998; Mansen *et al*., 1996). Specifically, clinical observations yielded a significant association between deleterious PPARγ mutations and Crohn's disease and the receptor was down-regulated in colons of patients with ulcerative colitis (Sugawara *et al*., 2005; Dubuquoy *et al*., 2003) . In addition, various studies have shown that PPARγ ligands are able to ameliorate acute inflammation, particularly in the colon (Katayama *et al*., 2003; Bassaganya-Riera *et al*., 2004). Though activation of this receptor represents a promising new therapy, the key mechanism of its anti-inflammatory effect is unknown. PPARγ is a receptor of endogenous lipids [i.e., prostaglandins or hydroxy-containing PUFA] that are produced during various homoestatic processes and has been shown to participate in a number of anti-inflammatory mechanisms including induction of anergy in inflammatory T-cells, enhanced regulatory T cell responses, suppression of inflammatory responses by macrophages, differentiation of macrophages towards an M2 phenotype, and suppression of T-cell effector responses (Odegaard *et al*., 2007; Lytle *et al*., 2005; Hontecillas & Bassaganya-Riera, 2007; Wohlfert *et al*., 2007; Odegaard *et al*., 2007; Odegaard *et al*., 2008; Mokdad *et al*., 2001; Desvergne & Wahli, 1999; Nesto *et al*., 2003). This work suggests that the specific mechanism underlying the PPARγ association with IBD prevention is PPARγ-mediated differentiation of M1 macrophages into M2 macrophages in the presence of anti-inflammatory cytokines IL-4, IL-13, IL-10, and TGF-β. Studies are underway to examine whether rescue from experimentally induced IBD can be achieved by treatment of mice with PPARγ ligands and subsequent differentiation of macrophages into an M2 phenotype.

Simulation results also indicate that increasing the rate at which activated macrophages revert back to a resting state can quell a chronic inflammatory response. Indeed, it is plausible that macrophage de-activation is a key function by which IL-10 is able to suppress IBD experimentally (Lang *et al*., 2002; Strober *et al*., 2002). The model, therefore, predicts that depriving the system of chemokines and cytokines that allow macrophages (both M1 and M2 alike) to stay activated should allow recovery from inflammation. This prediction may be tested by experiments in which mice experiencing chronic colitis are rescued by administration of chemokine inhibitors through various techniques (i.e. competitive inhibition with receptor antibodies, knockout mice, siRNA experiments), removing their ability to prolong the activation state.

In our model, active Tr effector activity included secretion of de-activating cytokines, meant to represent characteristic secretion of IL-10, and increased affinity for antigen-presenting cells coupled with an ability to deactivate effector dendritic cells upon contact (Onishi *et al*., 2008). Although activated CD25+ natural T-regulatory cells are associated with rescue from

colitis, presence of Tr did not have an impact on altering the course of immunopathogenesis or recovery in our system. It did, however, affect the length of the recovery period. This surprising outcome could be explained by the fact that induced T-regulatory cells are the main effectors behind these *in vivo* observations. Alternatively, the most effective mechanism by which Tr prevents, or ameliorates, colitis may not have been correctly defined in this version of the model. These include other contact-dependent actions such as inhibition of IL-12 secretion and induction of cytolysis in inflammatory cells (Shevach, 2002). Future versions of the model will also include alternative routes of activated natural T-regulatory cell traffic, specifically stimulation of resting T-cells in the inductive site followed by migration to the effector site.

Previous models have demonstrated immune regulation of inflammation as a factor in clinical effects of specific bacteria such as *H. pylori* and tuberculosis (Wigginton & Kirschner, 2001; Blaser & Kirschner, 1999; Day *et al*., 2009). In this study we present an abstract model of the gut mucosal immune system that incorporates regulatory mechanisms of both adaptive and innate immunity, multi-location migration of cells, and cross talk between antigen presenting cells and T-cells. The goal was to specify the immune cells that are upholding a pathogenic immune response to a non-pathogenic bacterial population. Some drawbacks to the mathematical approach taken here is that articulating the system in to ordinary differential equations (ODEs) can only capture the dynamics of each cell population as a whole assuming deterministic, average behavior by each individual cell. However, biological systems are known to act stochastically due to attributes, such as cytokine secretion and association time with stimulating factors, that vary widely across individual cells belonging to the same population. Additionally, the randomness introduced by cell movement leads to non-uniform distribution across single tissue sites. Because of ODE-induced assumptions of determinism and homogeneity, that are surely violated by the system in reality, dynamics predicted by an ODE model may not accurately reflect those seen in nature. In cases where such randomness, introduced by individual behavior, is believed to significantly affect the outcome of the system another approach, such as individual or agent based models (ABM), may be more appropriate (Bauer A., 2009).

While modeling approaches cannot replace traditional experimentation, they provide a conceptual framework for organizing existing data and focusing experiments through formulation of novel hypotheses. Thus, computer models of the immune system become necessary tools for tracing data gathered and mechanisms elucidated at the molecular and cellular levels back into an *in vivo* setting. The high-level model presented here is general enough to apply to other relevant mucosal sites including lungs, genital tract, and nasal passages with minor modifications and is useful for identifying the critical motifs of complex mucosal immunity that warrant more detailed investigation.

Future work will include a higher resolution exploration of the mechanisms identified here including specific cytokine populations and strain-specific responses to commensal and pathogenic bacteria by immune cells in the gut. In addition, further estimation and calibration carried out in COPASI with this model will be used to develop an ABM counterpart, the ENteric Immunity SImulator (ENISI). Similar experiments carried out with ENISI will illuminate the effect of allowing individual randomness on the behavior of the system as a whole.

Supplementary Material

Refer to Web version on PubMed Central for supplementary material.

Acknowledgments

We thank our external collaborators and members of the Network Dynamics and Simulation Science Laboratory (NDSSL) for their suggestions and comments. This work has been supported by NIH-NIGMS MIDAS project 5 U01 GM070694-05 and NIH MIDAS project 2U01GM070694-7.

6. Appendix A: Parameters

Table A.1 lists the values for parameters. When possible, constant values were assigned according to experimental data cited in the References column. For transition rates such as death, de-activation, and migration rates, measurements from the literature were in the form of an average lifespan or dwell time for an individual cell type in a particular location. In order to avoid introducing the complication of delay-differential equations, we used the common strategy of modeling cell death and movement as affecting a fixed proportion of cells in each time interval, resulting in an exponential distribution of lifetimes with the experimentally observed mean, x, or a half-life of $x \ln 2$.

In the case where measurement for a parameter was not found in the literature, the value was estimated from a range arbitrarily chosen or reasoned such that population dynamics fit the criteria for homeostasis listed in section 2.4 of the main text.

The unknown parameters ϵ_{BE} and ϵ_{EB}, representing the rate at which resting T-cells enter and exit the lamina propria, were formally optimized from the arbitrary range of 10^{-12} – 100. This was done by taking the ordinary least squares (OLS) estimate that minimized the net change in memory T-cell concentration before and after an inflammatory response. The OLS estimate was found with the particle swarm algorithm (Clerc & Kennedy, 2002) in COPASI.

'Estimation' in the Reference column indicates parameters estimated from a range where formal OLS analysis was not deemed necessary. For example, λ_c, the secretion rate assigned to both activating and de-activating cytokines, was not possible to gather from the literature as each group represents numerous cytokines that are secreted at different rates in reality. In fact, even secretion of a single type of cytokine is highly variable among individual cells of the same population. Acknowledging this fact, we sought to merely make the amount of activating (Ca) and de-activating cytokine (Cd) populations proportional to the concentrations of the cells that produce them. We initially assigned λ_c an arbitrary value of 0.25 per 6 hours corresponding to 1 per day. The cytokine degradation rate, μ_c, was then assigned the value of 0.075 for an average lingering period of 3 days in the extracellular environment. These values yielded the desired dynamics and sensitivity analysis showed them to not be highly influential on the system. Hence, their values were not modified. The same challenge was met in determining the value for ϵ_r, the rate of resting immune cell recruitment by Ca. This is also an artifical parameter given that, in reality, each cell type is recruited by different cytokines grouped in the Ca population at different rates. ϵ_r was initially assigned a value of 1 and then increased by a factor of 10 until we observed complete elimination of bacteria from the LP.

The parameters y_ϵ and q of the bacterial migration function, ϵ_{LE}, were initially set to 1. y_ϵ was then increased by 1 and q decreased by a factor of 10 until bacterial migration to the LP was detected in conjunction with inflammatory conditions, $C_a^E = 2.7 \cdot 10^8/mL$ and $E + E_p = 5.1 \cdot 10^3/mL$, yet not upon recovery, $C_a < 10/mL$ and $E + E = 10^4/mL$.

As explained in the main text, the rate of activated macrophage reversion to a resting state, ν_{M0}, is set to 0. This is because a value could not be found in the literature as the actual rate is based on numerous chemical factors not included in the model. A value of 0 resulted in experimentally predicted inflammation cessation in the validation step. For this reason we did not feel justified in applying an arbitrarily positive value to this parameter.

The bacterial competition coefficient, γ, was assigned a range of $10^{-15} - 10^{-10}$ allowing the term γB_c^L to evaluate to $0.001 - 100$ in equation 6 under the initial conditions of B_c^L concentration being $10^{12}/mL$. The value $2 \cdot 10^{-12}$ was then chosen as the maximum value that resulted in noticeable depletion of the foreign bacterial population, starting at a concentration of $10^8/mL$, in the presence of commensal bacteria (described in Equations 31 and 32), but without complete decimation in absence of immune cells.

In other cases we were able to take a more analytical approach to determining parameter ranges based on the dynamics desired. For example, the chosen range for the rate at which epithelial cells transition to pro-inflammatory epithelial cells, ν_{EC}, was based on the fact that for recovery to be seen following the inflammation-driven elimination of pathogenic bacteria, the normal epithelial cell population could not be lowered to 0, inducing the constraint $\nu_{EC} EC_a^E < 10^4/mL$ in equations 7 and 8. We predicted that C_a^E levels should reach a peak population on the order of 10^8, the level of T-helper cells measured in tissue (Haase, 1999;Hontecillas *et al*., 2005). Given that $E = 10^4/mL$ and $C_a^E = 10^8/mL$, approximately, at their peak concentrations, 10^{-8} was chosen as the maximum value for ν_{EC}. For this reason it was assigned the range $10^{-8} - 10^{-10}$. The value $5 \cdot 10^{-9}$ resulted in the characteristic recovery of epithelial cells after a transient decline coinciding with inflammation as seen in Figure 3B. The constraint for the rate of epithelial cell death by activating cytokines, μ_{CE} in equation 7, is that it must be less than ν_{CE}. For this reason it was assigned the value of $5 \cdot 10^{-10}$.

'Approximated' indicates that values were not estimated from a range nor based on values found in the literature directly, but were reasoned based on knowledge of the system.

For example, the cell contact rates k and k_L were initially assigned the value 10^{-12} under the assumption that each cell has an approximate volume of $1\mu m^3$. The parameter k was then estimated from this base value by increasing its value to 10^{-11}, which yielded complete bacterial elimination from the lamina propria when coupled with the parameter ϵ_r=100. As mentioned in the main text, the rate of contact between natural T-regulatory cells and antigen presenting cells, k_T, was then assigned to be greater than k following the observation that T-regulatory cells have higher affinity for dendritic cells than conventional T-cells (Onishi *et al*., 2008).

The birth rate of non-specific bacteria, λ_b, is based on the assumption that bacteria would double in the lumen every 6-12 hours in anaerobic conditions such as exist in the colon. The death rate μ_b was then calculated to uphold a population of approximately $10^{12}/mL$ based on the accepted concentration of bacteria in the colonic lumen (Artis, 2008).

The death rate of macrophages can be tissue specific and depend on the chemical environment. We assumed this lifespan to be 1 month corresponding to the parameter μ_m.

The parameter ν_T, the fraction of T-cells that become memory T-cells, was estimated to be approximately 1/500 based on the observation that one T-cell proliferates to approximately 500 clones (Geginat *et al*., 2003) and atleast one of those clones will be a memory T-cell.

The fraction of inflammation-inducing bacteria of the microflora, ν_{Bc}, was assumed to be 0 under the assumption that a healthy individual has only a negligible quantity of pathogenic bacteria in the colon at any given time.

The parameters λ_m, λ_d, λ_{dl}, ϵ_{LE}, ν_{12}, and ν_{21} are not constant but rather are determined by their corresponding equations.

The unit t refers to time units, which was approximated to 6 hours for parameter assignment. The units D, M, T, and C refer to active dendritic cells, macrophages, T-cells, and cytokines irrespective of their inflammatory/regulatory status. B refers to bacteria.

Table 1. A.1

Parameter values

Symbol	Description	Value	Reference
Birth/death			
λ_t	inflow rate of naive T-cells	$3 \cdot 10^7\ cells \cdot t^{-1}$	(Janeway *et al*., 2001)
λ_c	rate of cytokine production	$0{:}25 cells^{-1} \cdot t^{-1}$	estimated
λ_m	rate of M_0 creation	$M_0^E k B_c^E - \nu_M 0\left(M_1^E + M_2^E\right) + \mu_m M_0^E cells \cdot t^{-1}$	
λ_d	rate of D_i^E creation	$D_i^E\left(k B_c^E + \mu_{di}\right) cells \cdot t^{-1}$	
λ_{dl}	renewal rate of D_i^L	$D_i^L \left(k_L\ B_c^L + \mu_{di}\right) cells \cdot t^{-1}$	
λ_E	birth rate of epithelial cells	$2 \cdot E^{-1}$	(Kelly *et al*., 2004)
λ_b	birth rate of bacteria	$2 \cdot B^{-1}$	approximated
μ_t	removal rate of T_n	$0.25 \cdot t^{-1}$	(Janeway *et al*., 2001)
μ_T	rate of active T-cell deactivation	$0.05 \cdot t^{-1}$	(Janeway *et al*., 2001)
μ_c	rate of cytokine degradation	$0.075 \cdot t^{-1}$	estimated
μ_m	death rate of macrophages	$0.0075 \cdot t^{-1}$	approximated
μ_{di}	death rate of immature dendritic cells	$0.0006 \cdot t^{-1}$	(Kamath *et al*., 2002)
μ_d	dendritic cell death rate	$0.12 \cdot t^{-1}$	(Lanzavecchia & Sallusto, 2001)
μ_E	epithelial cell death rate	$0.5 \cdot t^{-1}$	(Kelly *et al*., 2004)
μ_{ce}	death rate, E by inflammatory factors	$5 \cdot 10^{-10} C^{-1} \cdot t^{-1}$	estimated
μ_b	death rate, bacteria	$1 \cdot t^{-1}$	(Artis, 2008)
p_t	T-cell proliferation rate from T_n, T_C	$0.122 \cdot t^{-1}$	(Swerdlin *et al*., 2008)
p_T	T-cell proliferation rate from TE	$0.03 \cdot t^{-1}$	(Sallusto *et al*., 2004)
p_{Tr}	proliferation rate, T_r	$0.05 \cdot t^{-1}$	(Janeway *et al*., 2001)
ϕ_E	crowding co-efficient, epithelial cells	0.00015	(Artis, 2008)
ϕ_b	crowding co-efficient, bacterial cells	1.9^{-12}	(Artis, 2008)
γ	competition coefficient, bacteria	2^{-12}	estimated
Migration			
ϵ_r	recruitment rate	$100 cells \cdot C^{-1} \cdot t^{-1}$	estimated
ϵ_{IE}	cell migration rate, inductive site to effector site	$0.125 \cdot t^{-1}$	(Janeway *et al*., 2001)

Symbol	Description	Value	Reference
ϵ_{EI}	cell migration rate, effector site to in- ductive site	$0.25 \cdot t^{-1}$	(von Andrian & Mempel, 2003)
ϵ_{LE}	bacteria migration rate, lumen to ef- fector site	$\left(\frac{C_a^E}{qC_a^E + E + E_p}\right)^{y_\epsilon} cells\, t^{-1}$	
y_ϵ	parameter of ϵ_{LE}	4	estimated
q	parameter of ϵ_{LE}	0.0001	estimated
ϵ_{BE}	inflow rate, blood to effector site	$0.025 \cdot t^{-1}$	optimized
ϵ_{EB}	outflow rate, effector site to blood	$10^{-10} \cdot t^{-1}$	optimized
Contact/interactions			
α_t	rate of naive T-cell stimulation by dendritic cells	$10^{-6} \cdot D^{-1}$	(Janeway *et al*., 2001)
α_T	rate of memory T-cell stimulation	$10^{-4}\,(D+M)^{-1}$	(Janeway *et al*., 2001)
ν_T	fraction of active T-cells that become memory T-cells	$0.002 \cdot T^{-1}$ 1	approximated
ν_{Bc}	fraction of B_r that induce inflamma- tory response	$0 \cdot B^{-1}$	approximated
ν_{M0}	rate of M_1 or M_2 reversion to M_o	$0 \cdot M^{-1}t^{-1}$	estimated
ν_{12}	rate that M_1 switches to M_2	$\left(\frac{\epsilon C_d}{\epsilon C_d + C_a}\right)^{y_\nu} \cdot M_1^{-1}\, t^{-1}$	
ν_{21}	rate that M_2 switches to M_1	$\left(\frac{C_a}{\epsilon C_d + C_a}\right)^{y_\nu} \cdot M_2^{-1}\, t^{-1}$	
ν_{EC}	rate that E switch E_p	$5 \cdot 10^{-9} \cdot C_a^{-1} \cdot t^{-1}$	
k	rate of contact between individuals	$10^{-11}\, cells \cdot 1^{-12}$	estimated
k_L	rate of contact between individuals specifically in the lumen	$10^{-12}\, cells \cdot 1^{-12}$	approximated
k_T	rate of contact between T_r and anti- gen presenting cells	$10^{-10}\, cells \cdot 1^{-10}$	approximated

Table 2. A.2

Population levels in homeostasis

Symbol	Description	Initial concentration
Inductive site		
T_n	Naive CD4+ T-cells	$1.2 \cdot 10^8$(Haase, 1999)
T_C	CD4+ Central Memory T-cells	$1.2 \cdot 10^8$
T_h^I	Active CD4+ T helper cells	0

Symbol	Description	Initial concentration
T_i^I	Induced T regulatory cells	177
T_r^{I*}	Active natural T regulatory cells	63
C_a^I	Activating cytokines	0
C_d^I	Deactivating cytokines	$1.6218 \cdot 10^7$
D_e^I	Effector dendritic cells	0
D_t^I	Tolerogenic dendritic cells	$4.39 \cdot 10^6$(Catron *et al*., 2004)
D_a^I	Anergic dendritic cells	0
Effector site		
T_E	CD4+ Effector T-cells	$9.3 \cdot 10^7$
T_h^E	Active CD4+ T helper cells	0
T_i^E	Induced T regulatory cells	1117.25
T_r^{E*}	Active natural T regulatory cells	3
T_r^E	Resting natural T regulatory cells	$2.99 \cdot 10^7$
C_a^E	Activating cytokines	0
C_d^E	Deactivating cytokines	$7.02 \cdot 10^6$
M_0^E	Undifferentiated macrophages	$1.2 \cdot 10^8$
M_1^E	Activating macrophages	0
M_2^E	Deactivating macrophages	0
D_i^E	Immature dendritic cells	$1.2 \cdot 10^8$(Hogue *et al*., 2008)
D_e^E	Effector dendritic cells	0
D_t^E	Tolerogenic dendritic cells	$2.105 \cdot 10^6$
E	Epithelial cells	10^4(Kelly *et al*., 2004)
E_p	Pro-inflammatory epithelial cell	0
B_c^E	Commensal bacteria	0
B_f^E	Foreign bacteria (Non-commensal)	0
Lumen		
B_c^L	Commensal bacteria	$5.26 \cdot 10^{11}$(Artis, 2008)
B_f^L	Foreign bacteria (Non-commensal)	$5.26 \cdot 10^{11}$(Artis, 2008)

Symbol	Description	Initial concentration
D_i^L	Immature dendritic cells that extend to the lumen	$1 \cdot 10^6$

7. Appendix B: Variable concentrations in homeostasis

Table A.2 lists the concentrations of variables in steady state, representing homeostasis prior to addition of pathogenic bacteria, as in the validation step, or any changes in the v_{Bc} parameter. Included are references to experimental measurements in agreement with the steady-state values. The steady-state was obtained by setting initial values of all active, inflammatory cells and activating cytokines to 0 and regulatory cell types in the lamina propria to 0.1. Resting cells were assigned initial values reflecting those found in the literature. Specifically, the effector memory T-cell concentration was intially $5.7 \cdot 10^7$, resting natural T-regulatory cell concentration was $9.3 \cdot 10^6$, and that of residential bacteria was set to 10^{10}. The immature dendritic cell population was assigned an initial concentration of $1.2 \cdot 10^8$, a value taken from a previously published model of dendritic cell activation and migration (Hogue *et al*., 2008). We then assumed approximately the same concentration for resting macrophages. Assumptions and approximations used in calculating target concentrations from patient data were that the average body contains 700g of lymphoid tissue, an approximation first used by Haase et al. (Haase, 1999), that 1g of tissue=1mL and 1mL of tissue=$1cm^3$. All concentrations are in units of mL^{-1}

References

Artis D. Epithelial-cell recognition of commensal bacteria and maintenance of immune homeostasis in the gut. Nat Rev Immunol 2008;8(6):411–20. [PubMed: 18469830]

Asano M, Toda M, Sakaguchi N, Sakaguchi S. Autoimmune disease as a consequence of developmental abnormality of a t cell subpopulation. Journal of Experimental Medicine 1996;184(2):387–396. [PubMed: 8760792]

Asseman C, Mauze S, Leach MW, Coffman RL, Powrie F. An essential role for interleukin 10 in the function of regulatory t cells that inhibit intestinal inflammation. J Exp Med 1999;190(7):995–1004. [PubMed: 10510089]

Barba G, Rebouissoux L, Le Bail B, Lamireau T. [recurrent pancreatitis revealing crohn's disease]. Arch Pediatr 2002;9(10):1053–5. [PubMed: 12462837]

Bassaganya-Riera J, Reynolds K, Martino-Catt S, Cui Y, Hennighausen L, Gonzalez F, Rohrer J, Benninghoff AU, Hontecillas R. Activation of ppar gamma and delta by conjugated linoleic acid mediates protection from experimental inflammatory bowel disease. Gastroenterology 2004;127(3): 777–91. [PubMed: 15362034]

Bauer A, Beauchemin C, P. A. Agent-based modeling in host-pathogen systems: the successes and challenges. Information Sciences 2009;179:1379–1389. [PubMed: 20161146]

Blaser MJ, Kirschner D. Dynamics of helicobacter pylori colonization in relation to the host response. Proc Natl Acad Sci U S A 1999;96(15):8359–64. [PubMed: 10411880]

Braverman IM. Skin signs of gastrointestinal disease. Gastroenterology 2003;124(6):1595–614. [PubMed: 12761719]

Catron DM, Itano AA, Pape KA, Mueller DL, Jenkins MK. Visualizing the first 50 hr of the primary immune response to a soluble antigen. Immunity 2004;21(3):341–347. [PubMed: 15357945]

Cho JH. The genetics and immunopathogenesis of inflammatory bowel disease. Nat Rev Immunol 2008;8 (6):458–66. [PubMed: 18500230]

Clerc M, Kennedy J. The particle swarm - explosion, stability, and convergence in a multidimensional complex space. Ieee Transactions on Evolutionary Computation 2002;6(1):58–73.

Day J, Friedman A, Schlesinger LS. Modeling the immune rheostat of macrophages in the lung in response to infection. Proc Natl Acad Sci U S A 2009;106(27):11246–51. [PubMed: 19549875]

Desvergne B, Wahli W. Peroxisome proliferator-activated receptors: nuclear control of metabolism. Endocr Rev 1999;20(5):649–88. [PubMed: 10529898]

Dubuquoy L, Jansson EA, Deeb S, Rakotobe S, Karoui M, Colombel JF, Auwerx J, Pettersson S, Desreumaux P. Impaired expression of peroxisome proliferator-activated receptor gamma in ulcerative colitis. Gastroenterology 2003;124(5):1265–76. [PubMed: 12730867]

Geginat J, Lanzavecchia A, Sallusto F. Proliferation and differentiation potential of human cd8+ memory t-cell subsets in response to antigen or homeostatic cytokines. Blood 2003;101(11):4260–6. [PubMed: 12576317]

Gordon S, Taylor PR. Monocyte and macrophage heterogeneity. Nat Rev Immunol 2005;5(12):953–64. [PubMed: 16322748]

Haase AT. Population biology of hiv-1 infection: viral and cd4(+) t cell demographics and dynamics in lymphatic tissues. Annual Review of Immunology 1999;17:625–656.

Hogue IB, Bajaria SH, Fallert BA, Qin S, Reinhart TA, Kirschner DE. The dual role of dendritic cells in the immune response to human immunodeficiency virus type 1 infection. J Gen Virol 2008;89(Pt 9): 2228–39. [PubMed: 18753232]

Hontecillas R, Bassaganya-Riera J. Peroxisome proliferator-activated receptor gamma is required for regulatory cd4+ t cell-mediated protection against colitis. J Immunol 2007;178(5):2940–9. [PubMed: 17312139]

Hontecillas R, Bassaganya-Riera J, Wilson J, Hutto DL, Wannemuehler MJ. Cd4+ t-cell responses and distribution at the colonic mucosa during brachyspira hyodysenteriae-induced colitis in pigs. Immunology 2005;115(1):127–35. [PubMed: 15819705]

Hoops S, Sahle S, Gauges R, Lee C, Pahle J, Simus N, Singhal M, Xu L, Mendes P, Kummer U. Copasi–a complex pathway simulator. Bioinformatics 2006;22(24):3067–74. [PubMed: 17032683]

Iwasaki A. Mucosal dendritic cells. Annual Review of Immunology 2007;25:381–418.

Janeway, C.; Travers, P.; Walport, M.; Shlomchik, M. Immunobiology: The immune system in health and disease. 5 edition. Garland Publishing; 2001.

Jonasson R, Andersson M, Rasback T, Johannisson A, Jensen-Waern M. Immunological alterations during the clinical and recovery phases of experimental swine dysentery. J Med Microbiol 2006;55 (Pt 7):845–55. [PubMed: 16772410]

Junt T, Moseman EA, Iannacone M, Massberg S, Lang PA, Boes M, Fink K, Henrickson SE, Shayakhmetov DM, Di Paolo NC, van Rooijen N, Mempel TR, Whelan SP, von Andrian UH. Subcapsular sinus macrophages in lymph nodes clear lymph-borne viruses and present them to antiviral b cells. Nature 2007;450(7166):110–4. [PubMed: 17934446]

Katayama K, Wada K, Nakajima A, Mizuguchi H, Hayakawa T, Nakagawa S, Kadowaki T, Nagai R, Kamisaki Y, Blumberg RS, Mayumi T. A novel ppar gamma gene therapy to control inflammation associated with inflammatory bowel disease in a murine model. Gastroenterology 2003;124(5):1315–24. [PubMed: 12730872]

Lang R, Rutschman RL, Greaves DR, Murray PJ. Autocrine deactivation of macrophages in transgenic mice constitutively overexpressing il-10 under control of the human cd68 promoter. J Immunol 2002;168(7):3402–11. [PubMed: 11907098]

Lytle C, Tod TJ, Vo KT, Lee JW, Atkinson RD, Straus DS. The peroxisome proliferator-activated receptor gamma ligand rosiglitazone delays the onset of inflammatory bowel disease in mice with interleukin 10 deficiency. Inflamm Bowel Dis 2005;11(3):231–43. [PubMed: 15735429]

Mansen A, Guardiola-Diaz H, Rafter J, Branting C, Gustafsson JA. Expression of the peroxisome proliferator-activated receptor (ppar) in the mouse colonic mucosa. Biochem Biophys Res Commun 1996;222(3):844–51. [PubMed: 8651933]

Marzo AL, Klonowski KD, Le Bon A, Borrow P, Tough DF, Lefrancois L. Initial t cell frequency dictates memory cd8+ t cell lineage commitment. Nat Immunol 2005;6(8):793–9. [PubMed: 16025119]

Mohr E, Serre K, Manz R, Cunningham A, Khan M, Hardie D, Bird R, MacLennan C. Dendritic cells and monocyte/macropahges that create the il-6/april-rich lymph node microenvironments where plasmabasts mature. Journal of Immunology February;2009 182:2113–2123.

Mokdad AH, Ford ES, Bowman BA, Nelson DE, Engelgau MM, Vinicor F, Marks JS. The continuing increase of diabetes in the us. Diabetes Care 2001;24(2):412. [PubMed: 11213906]

Nesto RW, Bell D, Bonow RO, Fonseca V, Grundy SM, Horton ES, Le Winter M, Porte D, Semenkovich CF, Smith S, Young LH, Kahn R. Thiazolidinedione use, fluid retention, and congestive heart failure: a consensus statement from the american heart association and american diabetes association. Circulation october 7;2003 108(23):2941–8. 2003. [PubMed: 14662691]

Odegaard JI, Ricardo-Gonzalez RR, Goforth MH, Morel CR, Subramanian V, Mukundan L, Red Eagle A, Vats D, Brombacher F, Ferrante AW, Chawla A. Macrophage-specific ppargamma controls alternative activation and improves insulin resistance. Nature 2007;447(7148):1116–20. [PubMed: 17515919]

Odegaard JI, Ricardo-Gonzalez RR, Red Eagle A, Vats D, Morel CR, Goforth MH, Subramanian V, Mukundan L, Ferrante AW, Chawla A. Alternative m2 activation of kupffer cells by ppardelta ameliorates obesity-induced insulin resistance. Cell Metab 2008;7(6):496–507. [PubMed: 18522831]

Onishi Y, Fehervari Z, Yamaguchi T, Sakaguchi S. Foxp3(+) natural regulatory t cells preferentially form aggregates on dendritic cells in vitro and actively inhibit their maturation. Proceedings of the National Academy of Sciences of the United States of America 2008;105(29):10113–10118. 330BB Times Cited:23 Cited References Count:39. [PubMed: 18635688]

Ott SJ, Musfeldt M, Wenderoth DF, Hampe J, Brant O, Folsch UR, Timmis KN, Schreiber S. Reduction in diversity of the colonic mucosa associated bacterial microflora in patients with active inflammatory bowel disease. Gut 2004;53(5):685–93. [PubMed: 15082587] Ott SJ, Musfeldt M, Wenderoth DF, Hampe J, Brant O, Folsch UR, Timmis KN, Schreiber S. Research Support, Non-U.S. Gov't England Gut. Gut May;2004 53(5):685–93. [PubMed: 15082587]

Powrie F, Leach MW, Mauze S, Caddle LB, Coffman RL. Phenotypically distinct subsets of cd4+ t cells induce or protect from chronic intestinal inflammation in c. b-17 scid mice. Int Immunol 1993;5(11): 1461–71. [PubMed: 7903159]

Reder C. Metabolic control theory: a structural approach. J Theor Biol 1988;135(2):175–201. [PubMed: 3267767]

Riley JL, June CH, Blazar BR. Human t regulatory cell therapy: take a billion or so and call me in the morning. Immunity 2009;30(5):656–65. [PubMed: 19464988]

Rutgeerts P, Vermeire S, Van Assche G. Biological therapies for inflammatory bowel diseases. Gastroenterology 2009;136(4):1182–97. [PubMed: 19249397]

Sallusto F, Geginat J, Lanzavecchia A. Central memory and effector memory t cell subsets: function, generation, and maintenance. Annu Rev Immunol 2004;22:745–63. [PubMed: 15032595]

Shevach EM. Cd4+ cd25+ suppressor t cells: more questions than answers. Nat Rev Immunol 2002;2(6): 389–400. [PubMed: 12093005]

Spiegelman BM. Ppargamma in monocytes: less pain, any gain? Cell 1998;93(2):153–5. [PubMed: 9568708]

Stenson WF. Interleukin-4 hyporesponsiveness in inflammatory bowel disease: immune defect or physiological response? Gastroenterology 1995;108(1):284–6. [PubMed: 7806051]

Strober W, Fuss IJ, Blumberg RS. The immunology of mucosal models of inflammation. Annu Rev Immunol 2002;20:495–549. [PubMed: 11861611]

Sugawara K, Olson TS, Moskaluk CA, Stevens BK, Hoang S, Kozaiwa K, Cominelli F, Ley KF, McDuffie M. Linkage to peroxisome proliferator-activated receptor-gamma in samp1/yitfc mice and in human crohn's disease. Gastroenterology 2005;128(2):351–60. [PubMed: 15685547]

Swidsinski A, Ladhoff A, Pernthaler A, Swidsinski S, Loening-Baucke V, Ortner M, Weber J, Hoffmann U, Schreiber S, Dietel M, Lochs H. Mucosal flora in inflammatory bowel disease. Gastroenterology 2002;122(1):44–54. [PubMed: 11781279] Swidsinski, Alexander; Ladhoff, Axel; Pernthaler, Annelie; Swidsinski, Sonja; Loening-Baucke, Vera; Ortner, Marianne; Weber, Jutta; Hoffmann, Uwe; Schreiber, Stefan; Dietel, Manfred; Lochs, Herbert. United States Gastroenterology. Gastroenterology Jan;2002 122(1):44–54. [PubMed: 11781279]

Uhlig HH, Coombes J, Mottet C, Izcue A, Thompson C, Fanger A, Tannapfel A, Fontenot JD, Ramsdell F, Powrie F. Characterization of foxp3(+)cd4(+)cd25(+) and il-10-secreting cd4(+)cd25(+) t cells during cure of colitis. Journal of Immunology 2006;177(9):5852–5860. 097VN Times Cited:81 Cited References Count:45.

Walker LS, Chodos A, Eggena M, Dooms H, Abbas AK. Antigen-dependent proliferation of cd4+ cd25 + regulatory t cells in vivo. J Exp Med 2003;198(2):249–58. [PubMed: 12874258]

Wigginton JE, Kirschner D. A model to predict cell-mediated immune regulatory mechanisms during human infection with mycobacterium tuberculosis. J Immunol 2001;166(3):1951–67. [PubMed: 11160244]

Wohlfert EA, Nichols FC, Nevius E, Clark RB. Peroxisome proliferator-activated receptor gamma (ppargamma) and immunoregulation: enhancement of regulatory t cells through ppargamma-dependent and -independent mechanisms. J Immunol 2007;178(7):4129–35. [PubMed: 17371968]

Yang R, Han X, Uchiyama T, Watkins SK, Yaguchi A, Delude RL, Fink MP. Il-6 is essential for development of gut barrier dysfunction after hemorrhagic shock and resuscitation in mice. Am J Physiol Gastrointest Liver Physiol 2003;285(3):G621–9. [PubMed: 12773301]

Yona S, Gordon S. Inflammation: glucocorticoids turn the monocyte switch. Immunol Cell Biol 2007;85 (2):81–2. [PubMed: 17242692]

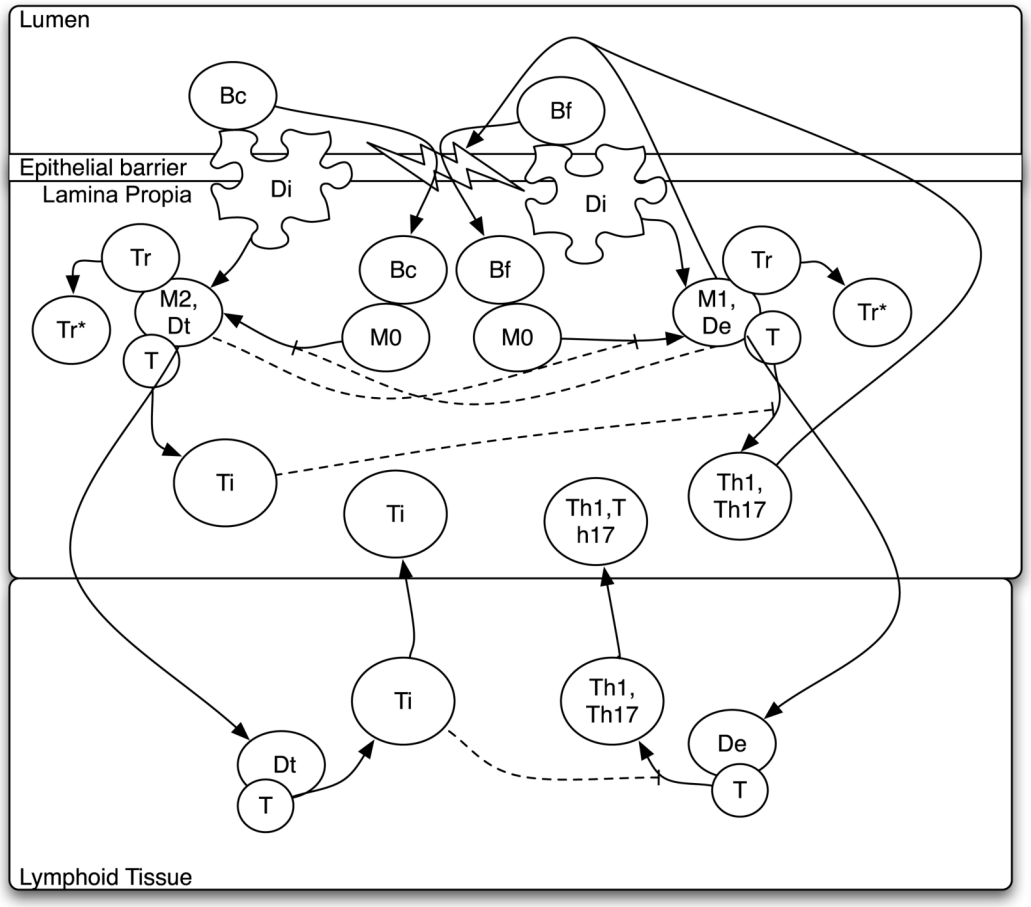

Figure 1.

Biological model of crosstalk between inflammatory and regulatory pathways in the gut. Solid lines represent either a reaction that induces cell differentiation from one type to another or the promotion by a cell type of a particular reaction. Dotted lines represent an inhibitory effect of a cell type on an interaction. The inflammatory pathway (right) is triggered by pathogenic (foreign) bacteria, Bf, and the regulatory pathway (left) is triggered by residential (commensal) bacteria, Bc. Each is described in the text along with other abbreviations.

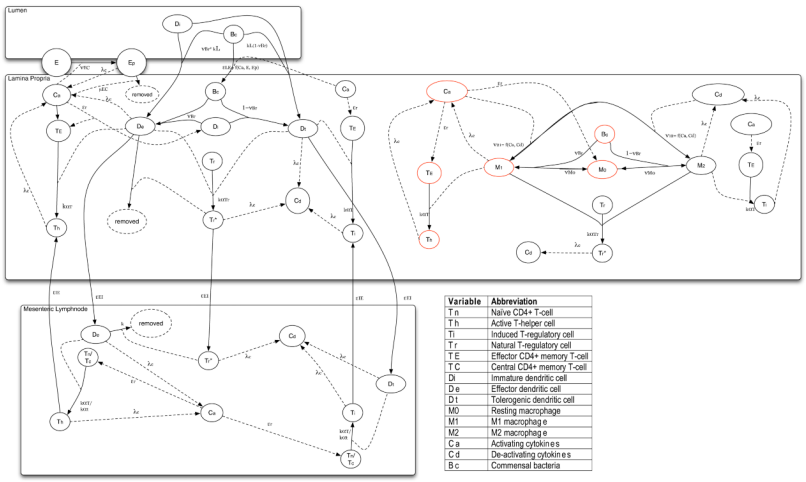

Figure 2.

Scheme of mathematical model of interacting populations represented explicitly in the model in the three location compartments: i) the lumen (top) ii) the lamina propria (middle), and iii) mesenteric lymph node (bottom). Solid arrows indicate cell transition from one population pool to another and are labelled with the rate or probability of this transition. Dashed arrows point from populations to the transition which they positively influence. The symbols for these parameters are described in Appendix A, table A.1. Red circles highlight the specific positive feedback loop that drives exponential growth of the activating cytokine population and epithelial cell depletion in the IBD model where Bc is able to stimulate Di and M0 to inflammatory phenotypes, De and M1.

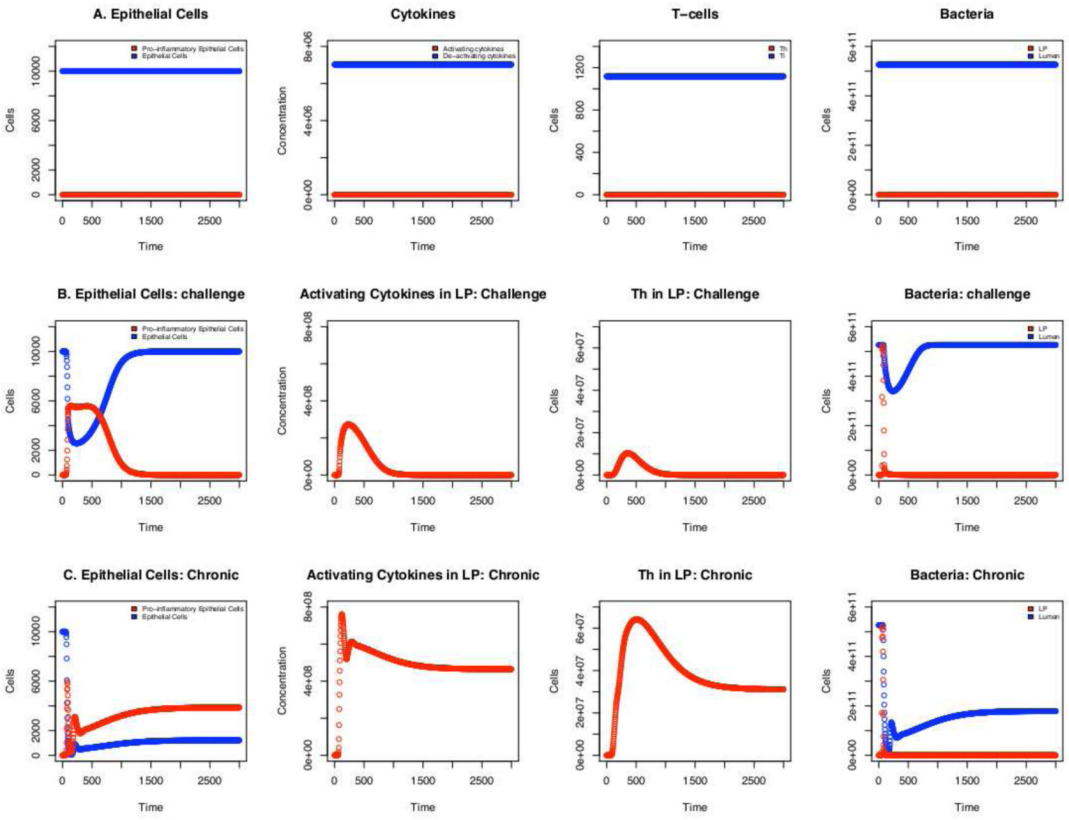

Figure 3.

Timecourse of fluctuations in select populations. A) Homeostasis: In the absence of an inflammatory response to bacteria in the lumen, the epithelial cell barrier remains intact and epithelial cells do not secrete inflammatory factors. Deactivating cytokines and induced T-regulatory cells are maintained at a basal level while activating cytokines and inflammatory T-helper cells are absent. Bacteria is compartmentalized to the lumen with no detectable invasion of the lamina propria (LP). B) Dysentery: The extended model that includes pathogenic bacteria that triggers an inflammatory response in macrophages and dendritic cells, epithelial cell erosion is seen as inflammatory markers rise in conjunction with translocation of bacteria into the LP. C) Chronic Inflammation: When a small fraction (0.0001) of bacteria in the lumen triggers an inflammatory response in macrophages and dendritic cells, the total epithelial cell population remains reduced in conjunction with elevated inflammatory markers and continued migration of bacteria into the lamina propria where it is readily eliminated by immune cells. This is typically seen in cases of inflammatory bowel disease.

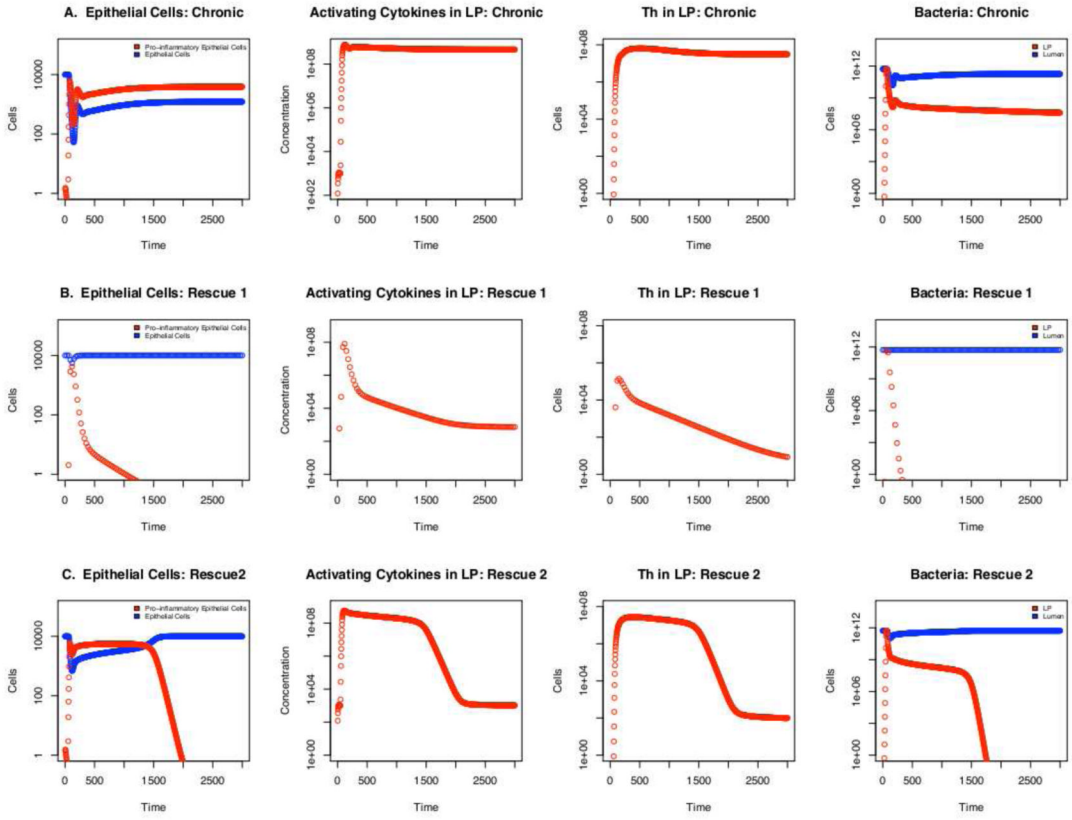

Figure 4.

Timecourse of fluctuations in select populations. The y-axis is in log scale to better compare population levels under chronic inflammation and rescue scenarios. A) Chronic inflammatory conditions of $v_{Bc} = 0.0001$, $\epsilon = 1$, and $v_{M0} = 0$. B) When the following parameter values are applied; $v_{Bc} = 0.0001$, $\epsilon = 2$, and $v_{M0} = 0$ requiring a lower de-activating cytokine concentration to induce transition from M1 to M2 in activated macrophages. This may also represent a higher activating cytokine threshold for inducing the opposite transition of M2 to M1. C) The following parameter values are applied; $v_{Bc} = 0.0001$, $\epsilon = 1$, and $v_{M0} = 0.015$ representing a system in which activated macrophages may become deactivated. As the value v_{M0} increases this recovery period is shortened (not shown).

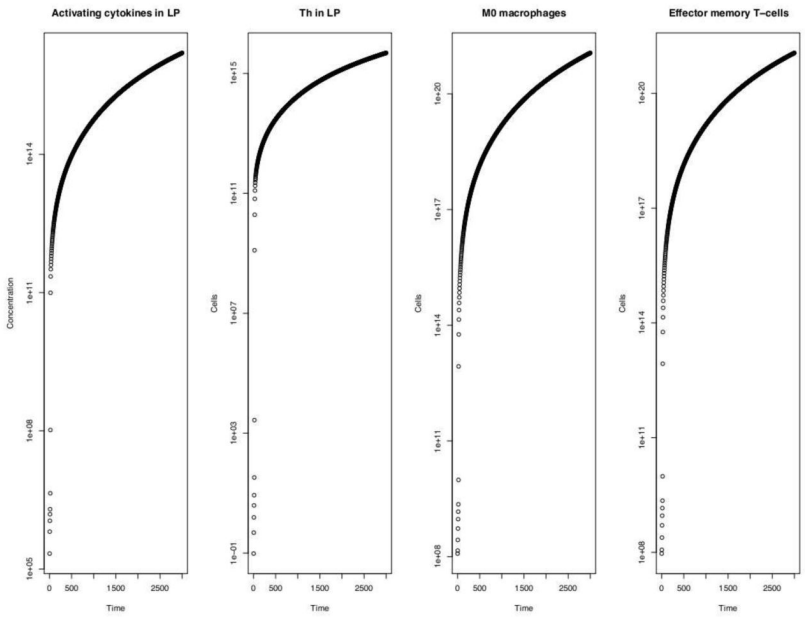

Figure5.
Timecourse of cell populations in the system that grow in proportion to the activating cytokine levels (far left) when $v_{Bc} \geq 0.01$. This indicates their critical roles in the positive feedback pathway described in section 3.3 of the main text.